Robust Power Aware Mobile Agent Tracking using an 802.15.4 Wireless Sensor Network. ⋆

Michael J. Walsh * **and Martin J. Hayes** *

* *Wireless Access Research Centre, University of Limerick, Limerick, Ireland (e-mail: michael.j.walsh@ul.ie; martin.j.hayes@ul.ie).*

Abstract: This work presents an experimental analysis for a lean power, 802.15.4 wireless sensor network based mobile agent tracking problem. A localization procedure is designed that robustly tracks a moving agent despite significant uncertainty existing on the received signal strength vector. The benefits of dynamic power control are considered at two separate levels within the network topology. Firstly, active management of the uplink connection between the stationary tracking reference nodes and a base station is critically assessed. The cost performance benefit that arises from the use of additional feedback bandwidth, where available, and also the design of effective time delay compensation is discussed within this paradigm. Secondly, an additional power control loop is presented where the effects of Raleigh fading and varying time delay on the uplink between mobile node and base station are major factors influencing system performance.

1. INTRODUCTION

The question of performance robustness appears to be a recurring theme in the Wireless Sensor Network (WSN) applications literature at the present time. In addition to reliability in terms of a lower bound on information, as opposed to merely data flow, within the network the need for an upper bound on power consumption in order to maximise operational longevity is invariably also a requirement. As a motivating example a scale model of a recent high profile safety critical fire-fighting deployment is considered, [Engineering and Magazine, 2007], wherein robots are used to ascertain possible dangers to human rescue teams. In this example robust performance is taken to mean that a lower bound on information flow from each robot is achieved despite the presence of gain bounded levels of interference on the robot basestation communications link. This work looks at how joint power and information flow control can be achieved in such an environment where significant output uncertainty exists. While the focus is on reliable information flow, active power management can mean that agents can be deployed for longer in the field. All the results presented herein are demonstrated using a practical short range 802.15.4 wireless network that is highly effective from a cost and performance perspective.

A localization algorithm is implemented wherein the position of an array of mobile agents is always known by at least one agent in the network. Thus, at any instant a possible exit path should be identifiable for every agent in the mesh. The robustness of the network that manages the information flow for the dynamic determination of this path is assessed. Clearly this type of robust performance is a prerequisite for any deployment of human teams on the site in question.

⋆ This work was partially supported by IRCSET Embark Initiative.

2. WIRELESS SENSOR NETWORK LOCALIZATION

In this scenario power control is implemented in conjunction with node localization, therefore the number of predefined useful localization techniques is limited by the requirement that transmit power remain at a fixed level. A variant of a class of localization strategies known as Ecolocation [Yedavalli et al., 2005] is utilized for this case study. This procedure is characterised by it's ease of implementation and is therefore suitable for the complex problem at hand.

Consider a mobile node MN, who's position is to be estimated and who's output power is time varying as a result of dynamic power management. To localize MN the distance between each grid point (i, j) in the localization area, and each reference node RN_k is calculated using:

$$d_{RN_k} = \sqrt{(x_{RN_k} - i)^2 + (y_{RN_k} - j)^2} \tag{1}$$

It is assumed the positions of all reference nodes $(x_{RN_k},\ y_{RN_k})$ are known. These values are stored in a matrix D^{ij}. The distances for each grid point (i, j) are arranged in descending order and their respective reference node numbers are then stored. Hence for the simple scenario in Fig. 1(a), the values [4 3 2 1] are stored in R^{ij}. Experimental real-time received signal strength indicator (RSSI) measurements, taken at MN are then arranged in descending order and their reference node numbers recorded and denoted by the vector $\overrightarrow{mn}$. Again, for the simple scenario in Fig. 1(b) the vector $\overrightarrow{mn}$ = [3 2 4 1]. An iterative algorithm then compares each element in R^{ij} to the sorted reference node vector $\overrightarrow{mn}$ and any match(es) is(are) recorded. It is assumed a larger transmission distance will lead to the largest amount of attenuation resulting in a lower RSSI value. This assumption is not straightforward, given that MN is likely to be moving it is quite likely to exhibit multipath fading. To address this constraint, each of the channels contains a filter that is designed to limit the effect

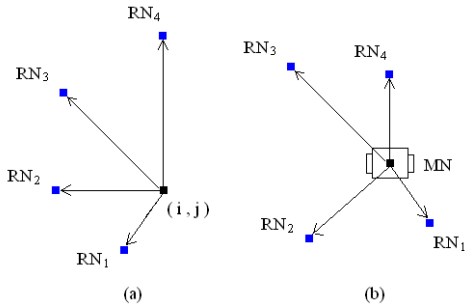

Fig. 1. The reference nodes RN_i are ordered dependant on distance in descending order. In (a) for instance this would be (RN_4 RN_3 RN_2 RN_1)

multipath fading within a dynamic localization procedure (see Fig. 2).

The estimated position of MN is directly related to the recorded match, from which the localised position can be determined based on a Least Square Estimate (LSE), [Feldmann et al., 2003]. Assuming the position of each reference node RN_k, $k \in 1..L$ is known to be $(x_{RN_k},\ y_{RN_k})$ and the distance to each node from the estimated position of MN is d_{RN_k}, then for any two reference nodes RN_i and RN_j the section boundaries can be computed to be:

$$d_{RN_i}^2 - d_{RN_j}^2 = (x_{MN} - x_{RN_i})^2 + (y_{MN} - y_{RN_i})^2$$
$$-(x_{MN} - x_{RN_j})^2 - (y_{MN} - y_{RN_j})^2 \quad (2)$$

where $p_{MN} = (x_{MN},\ y_{MN})^T$ is the estimated position of MN. p_{MN} can be calculated from:

$$H.p_{MN} = C \quad (3)$$

with

$$H = \begin{bmatrix} h_{x(2,1)} & h_{y(2,1)} \\ \vdots & \vdots \\ h_{x(L,1)} & h_{y(L,1)} \\ \vdots & \vdots \\ h_{x(L,L-1)} & h_{y(L,L-1)} \end{bmatrix},\ p_{MN} = \begin{bmatrix} x_{MN} \\ y_{MN} \end{bmatrix}$$

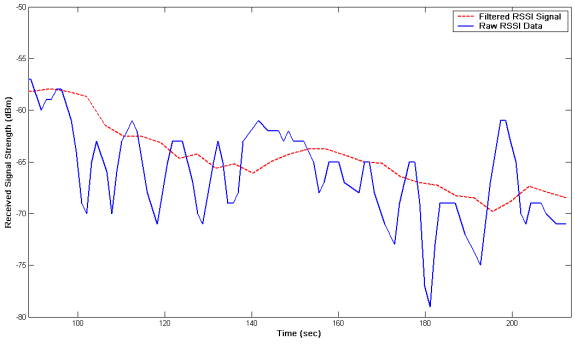

Fig. 2. Received Signal Strength (RSS) filtered to remove multipath effects.

$$C = \begin{bmatrix} c_{2,1} \\ \vdots \\ c_{L,1} \\ \vdots \\ c_{L,L-1} \end{bmatrix} \quad (4)$$

where

$$h_{x_{RN}}(i,j) = 2(x_{RN_j} - x_{RN_i})$$
$$h_{y_{RN}}(i,j) = 2(y_{RN_j} - y_{RN_i})$$

and

$$c_{i,j} = d_{RN_i}^2 - d_{RN_j}^2 + x_{RN_j}^2 - x_{RN_i}^2 - y_{RN_j}^2 - y_{RN_i}^2$$

The location estimation is then determined from:

$$p_{MN}^T = (H^T H)^{-1} H^T C \quad (5)$$

3. THE 802.15.4 WIRELESS CHANNEL MODEL

As mentioned previously, the 802.15.4 wireless protocol is adopted to verify our hypothesis. The Telos mote sensor node is a primary embedded platform using an 802.15.4 compliant transceiver. The Telos platform employs the CC2420 transceiver using the Direct Sequence Spread Spectrum (DSSS) technique to code the required data. Carrier Sensing Multiple Access/Collision Avoidance (CSMA/CA) is then used to transmit the coded packets. For controller synthesis a model of the 802.15.4 wireless channel is required, noting that a value in the linear scale is represented by $\bar{g}$ and g is it's corresponding value in dB namely $g = 10log_{10}\bar{g}$, where $\bar{g}(k)$ is a time-varying multiplicative power gain. The signal to interference plus noise ratio (SINR) of the i-th node for a network consisting of n nodes communicating with a base station is given by:

$$\bar{\gamma}_i(k) = \frac{\bar{p}_i(k)\bar{g}_i(k)}{\sum_{j \in \mathcal{Z}, i \neq j} \bar{q}_j(k)\bar{p}_j(k)\bar{g}_j(k) + \bar{n}_i(k)} \quad (6)$$

where $\bar{n}_i$ is the power of the white noise at the base station to which the i-th is communicating. $\sum_{j \in \mathcal{Z}, i \neq j} \bar{q}_j(k)\bar{p}_j(k)\bar{g}_j(k)$ is the sum of the interference from all nodes simultaneously communicating with the base station and $\mathcal{Z}$ is the set of all nodes interfering with node i. Here $\bar{q}(k)$ is a binary random variable modelling the CSMA/CA transmission attempts of the nodes. Therefore if a mobile node MN_j is transmitting it has $\bar{q}_j(k) = 1$ and $\bar{q}_j(k) = 0$ otherwise. Note that the probability $P_r(\bar{q}_j(k) = 1) = \alpha_i$ and accordingly the probability $P_r(\bar{q}_j(k) = 0) = 1 - \alpha_i$. Representing (6) in dB results in:

$$\gamma_i(k) = p_i(k) + g_i(k) - I_i(k) \quad (7)$$

A similar approach to [Ares et al., 2007] is used to directly estimated the SINR using the RSSI. A setpoint or reference RSSI value can thusly be selected and related directly to packet error rate (PER) as outlined in the 802.15.4 standard [Standard, 2006]. To expand, the bit error rate (BER) for the 802.15.4 standard operating at a frequency of 2.4GHz is given by:

$$BER = \frac{8}{15} \times \frac{1}{16} \times \sum_{k=2}^{16} -1^k \binom{16}{k} e^{20 \times SINR \times (\frac{1}{k} - 1)}, \quad (8)$$

and given the average packet length for this standard is 22 bytes, the PER can be obtained from:

$$PER = 1 - (1 - BER)^{PL} \tag{9}$$

where PL is packet length including the header and payload. Establishing a relationship between RSSI and SINR and subsequently PER can therefore help to pre-specify levels of system performance. From [Ares et al., 2007] the SINR is given by:

$$10log_{10}\bar{\gamma_i}(k) \approx RSSI_i(k) - n_i(k) - C - 30 \tag{10}$$

where the addition of the scalar term 30 accounts for the conversion from dBm to dB and C is the measurement offset assumed to be 45 dB. The SINR in dB is thus:

$$\gamma_i(k) = 10^{(RSSI_I(k) - n_i(k) - C - 30)/10}. \tag{11}$$

4. LOG LINEAR POWER CONTROL ALGORITHMS

Consider the arrangement of Fig. 3. The performance objective here is to measure the actual SINR $\gamma(k)$ and to compare it with a prescribed attainable target SINR value $\gamma_t(k)$. This target value is directly relatable to RSSI using equation (10). The controller outputs a value which in essence determines whether the mobile user increases or decreases its transmission power. A similar approach to [Gunnarsson et al., 1999] is adopted here with $G_i(q) = \frac{\beta}{q-1}$ representing the case where:

$$p_i(k+1) = p_i(k) + \beta e_i(k) \tag{12}$$

which is an integrating controller with $C_i\{e_i(k)\} = e_i(k)$. Assuming:

$$C(q) = \frac{\beta}{q-1},\ u_i = p_i,\ G_i\{p_i(k-n_p)\} = p_i(k-n_p) \tag{13}$$

is a more natural interpretation allowing for a number of different designs to be implemented as C_i. There are two important feedback classes that should be considered when implementing radio power control. The first is *information feedback*, as in (19) above, where exact measurements are fed back from the transmitter. In this instance the error is:

$$e_i(k) = \gamma_i^t - \gamma_i(k). \tag{14}$$

A second approach is *decision feedback* where the sign of the error alone is fed back resulting in:

$$s_i(k) = sign(\gamma_i^t - \gamma_i(k)) = sign(e_i(k)) \tag{15}$$

This method requires just one bit for signalling which is extremely bandwidth efficient. When utilizing decision feedback, as in [Salmasi and Gilhousen, 1991], the simple Integral (I) controller in (12) takes the form:

$$p_i(k+1) = p_i(k) + \beta s_i(k) \tag{16}$$

The controller in (18) above is often referred to as a *Fixed Step* size power law where the power $p_i(k)$ is increased or decreased by β depending on the sign of the error $e_i(k)$. An *Adaptive Step* size power control uses the same power control law as a fixed step approach (18), however the parameter β is updated depending on system requirements according to the following:

$$\beta(k) = [\alpha\beta^2(k-1) + (1-\alpha)\sigma_e^2]^{\frac{1}{2}} \tag{17}$$

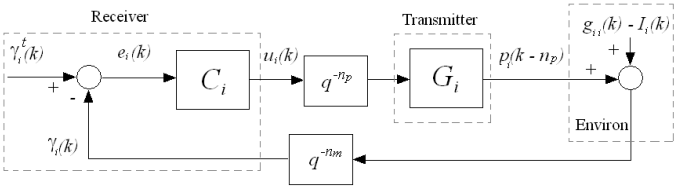

Fig. 3. Block diagram of the receiver-transmitter pair i when employing an SIR-based power controller

where as before σ_e is the sampled standard deviation of the power control tracking error and α is the forgetting factor, introduced to smooth a measured SINR signal that may be corrupted by noise.

4.1 Anti-Reset

To ensure the inherent hardware saturation limitations $[P_{min}, P_{max}]$ are not surpassed, Anti-Reset ([Astrom and Wittenmark, 1997]) is employed. This technique recomputes the integral output keeping the transceiver power of the system within it's operational constraints. A filter is used to ensure the anti-reset is not limited by short periods of saturation that may be introduced by noise. In essence an additional feedback path is added around the integrator to stabilize the integrator when the main feedback loop is effectively open due to saturation. Thus if the integrator state is $x_i(k)$ it is updated according to:

$$x_r(k) = x_i(k) + \frac{1}{T_t}(f(p_i(k)) - p_i(k)), \tag{18}$$

where the constraints $[P_{min}, P_{max}]$ are described by the static memoryless nonlinear function $f(.)$, $x_r(k)$ is the recomputed integrator state and T_t is a tracking parameter. Note that if no saturation exists $f(p_i(k)) = p_i(k)$, $x_r(k)$ is equal to $x(k)$. In general the smaller T_t is the quicker the reset, but it should be noted that this rule of thumb must be noise bandlimited.

4.2 Smith Prediction: Time Delay Compensation

Time delay imposes a severe performance constraint on the closed loop performance of a power aware network based application. One approach to the compensation of time delay systems, (particularly in the process industries), is through the use of a Smith predictor [Astrom and Wittenmark, 1997]. In essence the Smith Predictor is implemented as per the arrangement in Fig. 3 by:

$$\tilde{\gamma_i}(k) = \gamma_i(k) + p_i(k) - p_i(k - n_m - n_p) \tag{19}$$

where $\tilde{\gamma_i}(k)$ is an adjusted SINR measurement at the receiver.

5. PRACTICAL IMPLEMENTATION

The above control laws are now critically assessed using a wireless problem scenario that implements the agent localization procedure discussed earlier.

5.1 Experimental Setup

Consider the testbed in Fig. 4, consisting of nine fixed position reference Tmote Sky nodes, one base station (also

a Tmote sky device) and one mobile node. The mobile node was attached to a MIABOT Pro fully autonomous miniature mobile robot. The base station was connected directly, via usb connection, to a PC where the power aware localization algorithm was implemented. The motes are located $60cm$ apart covering in total an area of $1.8m^2$. As the application is entirely scalable no new point of principle arises in a full scale building wide deployment.

5.2 Localization

The localization technique was implemented as follows. The mobile node positioned on the MIABOT communicated information to each of the reference nodes. Upon receiving a packet from the mobile agent each reference node calculated the RSSI and once ten packets had arrived the recorded RSSI data was sent to the base station for processing. The RSSI data once received from all nine reference nodes was filtered to remove any multipath component which may in turn lead to erroneous results. The data was then arranged in descending order of magnitude and compared to the comparison matrix D^{ij} containing some 23409 elements and with a possible 2601 location matches. In this experiment D^{ij} contains samples taken at a spacing of $2cm$. The MIABOT was then programmed to travel a (random) route and the localization technique was engaged to record it's position at regular 5 second intervals. Results for one complete experiment are shown in Fig. 5, where the technique performs well, tracking the mobile node to within an error of $5.5cm$.

5.3 Power Control Observations

As the reference nodes are themselves wireless devices and are assumed to have limited available power, the performance objective at hand it is to keep nodes transmitting at as low a power as possible, thereby lengthening battery lifetime. Power control in this scenario is used to compensate for interference generated by surrounding nodes and other noise that may be exogenous to the system in question. Given the reference nodes and the base station are in situ, is no Rayleigh fading present at the receiver and therefore power control is more straightforward. To ensure that a reliable connection is maintained between the mobile node and the base station in this context,

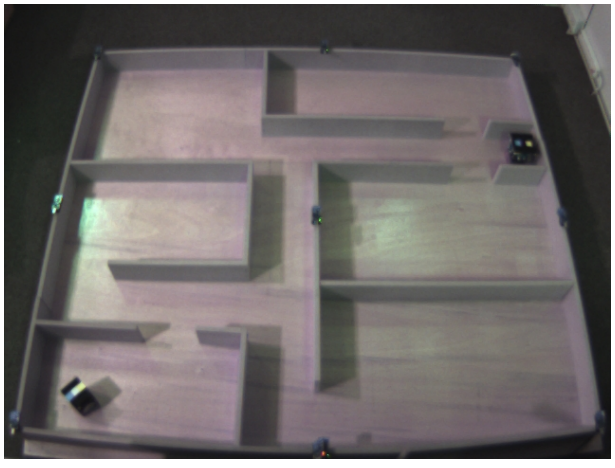

Fig. 4. Localization Experimental Set-up

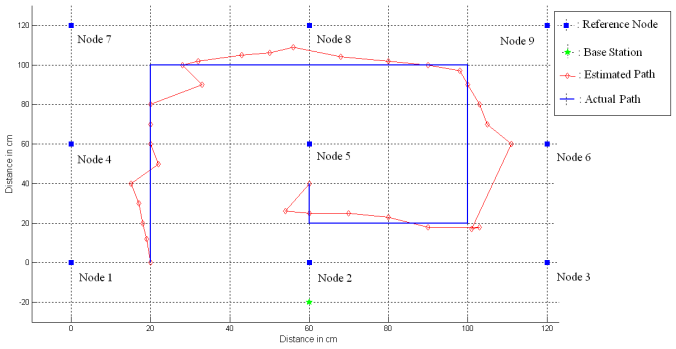

Fig. 5. Localization test results.

power control is implemented on the uplink connection. Uncertain factors that are considered in this scenario are the motion of the transmitter and hence a parameterised incorporation of multipath fading within the signal observed at the receiver. Sampling frequencies of $T_s = 1(sec)$ and $T_s = 5(sec)$ are selected for the mobile node and stationary reference nodes respectively. A target RSSI value of -55dBm is selected for the mobile node, guaranteeing a PER of $< 1\%$, verified using equations 8, 9 and 10. To optimize power consumption a setpoint of -65dBm is chosen for the reference nodes, assuming the absence of deep fading associated with mobility.

Reference Node Power Control: Each of the power control algorithms introduced in section 4 was tested in concert with the aforementioned localization procedure. For purposes of clarity only, links three, five and seven (see Fig. 5) are represented graphically in Fig. 6. Here, the results for fixed step power control represented by equation (18) are illustrated. The bottom of Fig. 6 shows the output power level (or controller actuator) value. This value is written to the CC2420 transceiver and represents the amplitude of the RF wave. Thus, the higher the value that is written to the transceiver the greater the RF wave amplitude and the more power consumed by the network. Clearly the distance from the base station directly also influences the output power level, with link 7 located furthest away, this node obviously needs to transmits at a higher power. The limiting effect of decision feedback in this context is noted at this point of the analysis.

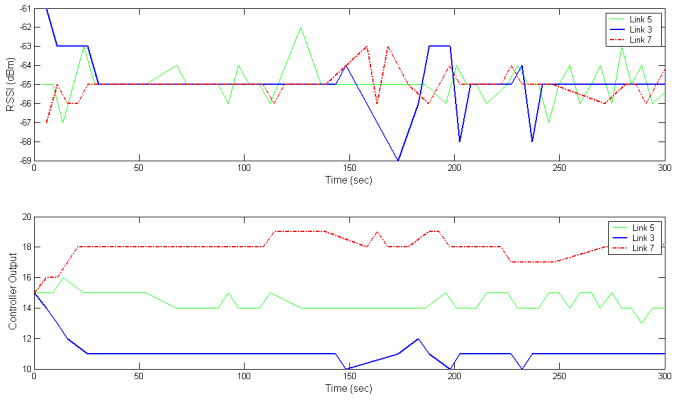

Fig. 6. Fixed Step Power Control (equation (25)) with $\beta = 1$. Where Link 3 is the thick line, Link 5 is the thin solid line and Link 7 is dashed line

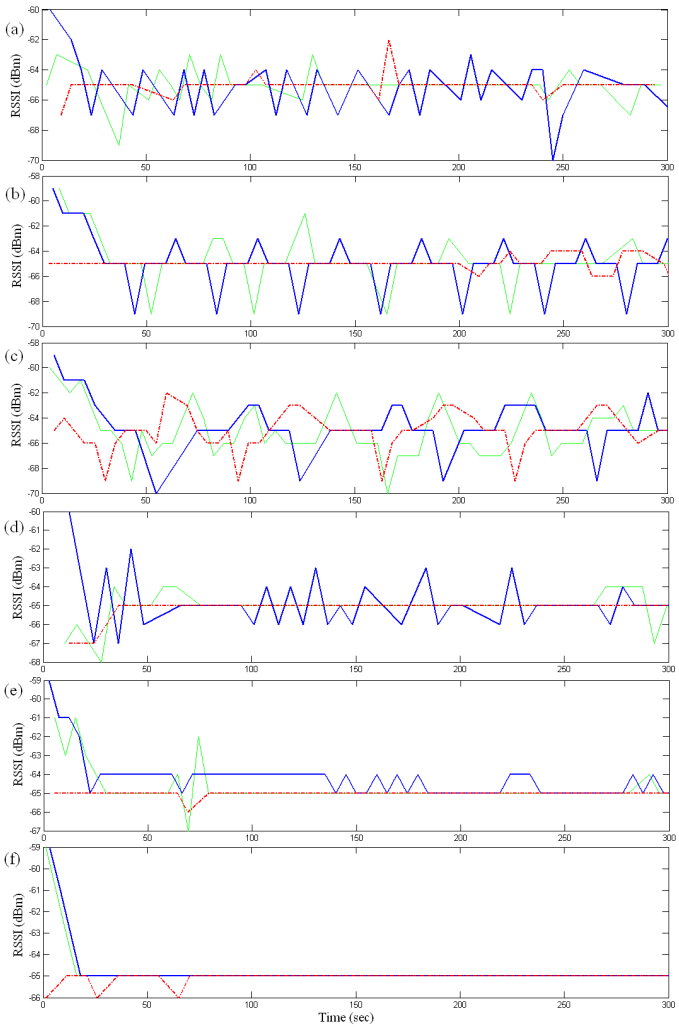

Fig. 7. Reference Node Power Control

Fig. 7 shows the system response for a number of other controller parameter values and configurations. Fig. 7(a) shows the fixed step size configuration with $\beta = 2$. The increased step size does not improve the system output and in fact when compared to Fig. 6 the response proves to be more oscillatory. In Fig. 7(b) the response shows improvement with a fixed step size $\beta = 1$ and Smith prediction with roundtrip delay assumed to be one. Increasing the step size to $\beta = 2$ with Smith prediction, shown in Fig. 7(c), as in the previous instance does not further improve the system performance and in fact as before a more oscillatory output is observed.

Adaptive step size power control, using equations (26) and (25) is implemented next and the response shown in Fig. 7(d) shows considerable improvement on the previous four configurations. The forgetting factor is set to 0.95 to help smooth the measured RSSI value and this explains the enhanced performance. In Fig. 7(e) information feedback is used to implement equation (19) using $\beta = 0.35$ as suggested by [Gunnarsson and Gustafsson, 2002]. The added flexibility associated with the use of information feedback is very apparent here. A significant improvement in tracking performance is observed with this scheme. To compensate for the effect of roundtrip delay, which here is nominally suggested to be one sampling period,

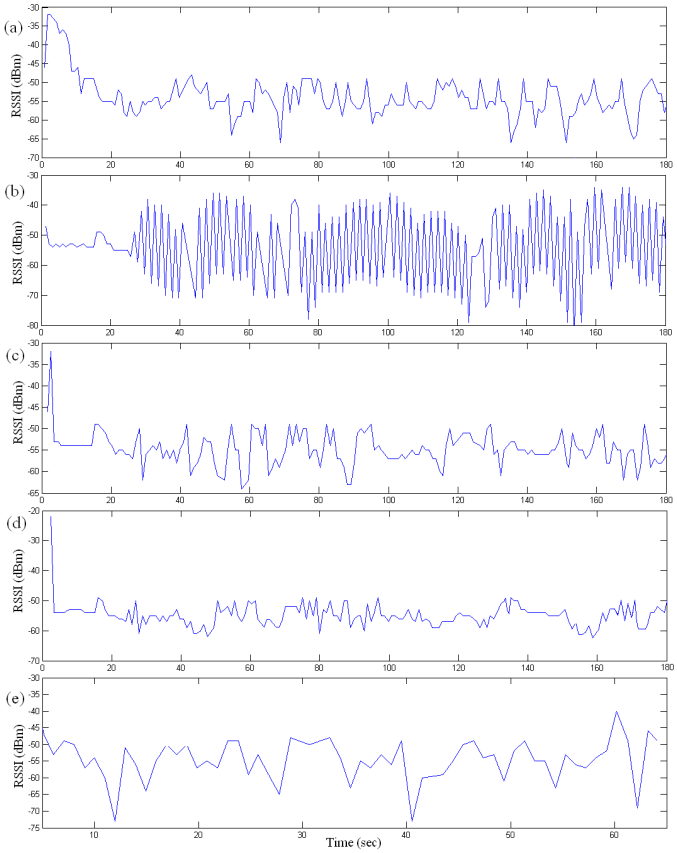

Fig. 8. Mobile Node Power Control

Smith prediction is added to the system. Clearly this configuration offers excellent nominal performance.

Mobile Node Power Control: As stated previously the difficulty in implementing power control for a mobile node is the presence of multipath fading in the received RSSI signal. With this in mind its seems natural to rule out decision feedback based control entirely unless is is impossible to do so, i.e. when limited bandwidth is available. To demonstrate why this is advisable, the configuration shown to perform best for the reference node power control using decision feedback was implemented on the uplink between the mobile node and the base station. The results are shown in Fig. 8(a) using a fixed step size approach with $\beta = 1$ and Smith prediction with a delay of one. Clearly decision feedback based control struggles to cope with the rapidly changing received signal. Adaptive step size power control again using a forgetting factor of 0.95 is in fact close to unstable in this experiment which may be explained by the inability of the controller to compensate for time delay.

Fig. 8(c) illustrates the system response using information feedback in equation (12) with $\beta = 0.35$, again taken from [Gunnarsson and Gustafsson, 2002] and with Smith prediction again assuming a nominal delay of one sample instant. In this instance the Smith predictor exhibits poor robustness properties as significant variability will now exist on the delay parameter for the mobile node. The most satisfactory response is now obtained using information feedback or equation (12), with $\beta = 0.35$ and shown in Fig. 8(d). It is important to note here the

speed at which the mobile node is travelling, (in this case the mobile node speed is $0.01m/sec$). As a result Rayleigh fading is not as pronounced as it would be for an agent moving with greater velocity. To characterise this effect, the same experiment is repeated with the mobile node moving at $0.05m/sec$. The results depicted in Fig. 8(e) show that the magnitude of the multipath effects is much more significant in this latter scenario. Note the characteristic deep fades that are far more obvious to the observer. The results do however clearly show that significant performance improvements can be achieved using power control to dynamically manage transmission output power level.

Power Efficiency To measure the power efficiency for the respective algorithms, the power efficiency for any one controller configuration is defined as the average power consumed by all motes operating using a particular power control algorithm for the duration of an experiment. For example 100% efficiency in this context would imply that all nodes are transmitting using their minimum output power setting and vice versa. Fig. 9 plots the percentage power efficiency for each of the reference node control configurations. In Fig. 9(a) 1 relates to fixed step power control with $\beta = 1$ or Fig. 6, 2 relates to fixed step with $\beta = 2$ or Fig. 7(a), 3 relates to fixed step with $\beta = 1$ and Smith prediction roundtrip delay = 1 or Fig. 7(b), 4 relates to fixed step with $\beta = 2$ and Smith prediction roundtrip delay = 1 or Fig. 7(c), 5 relates to adaptive control with forgetting factor = 0.95 or Fig. 7(d), 6 relates to information feedback with $\beta = 0.35$ or Fig. 7(e) and 7 relates to Information feedback $\beta = 0.35$ and Smith prediction roundtrip delay =1 or Fig. 7(f). In Fig. 8(b) 1 relates to fixed step with $\beta = 1$ or Fig. 8(a), 2 relates to adaptive control with forgetting factor = 0.95 or Fig. 8(b), 3 relates to information feedback $\beta = 0.35$ and Smith prediction roundtrip delay =1 or Fig. 8(c), 4 relates to information feedback with $\beta = 0.35$ or Fig. 8(d) and 5 relates to Information feedback with $\beta = 0.35$ with speed increased by a factor of 4 or Fig. 8(e).

It is noticeable that the mobile node power control algorithms have lower percentage power efficiency. This might seem strange, but if the path along which the mobile node moves during localization is examined it is clear that the distance from the base station is never as large as the distance to the base station for reference nodes 7,8 and 9 and for much of the experiment reference nodes 4,5 and 6 (see Fig. 5). Therefore it can be expected that decreased power efficiency will be observed for the reference nodes when averaged over all nine nodes.

6. CONCLUSIONS

This work has examined how power control can be implemented successfully in a power aware 802.15.4 wireless sensor network. Information flow in the network was assessed using a localization procedure that tracks a mobile agent using filtered signal strength measurements. The robustness of a localization procedure was examined in conjunction with several power control algorithms used on the link. Best nominal performance was achieved through the use of information feedback together with a Smith predictor. Robustness to Raleigh fading was a focus in this work and, taken in conjunction with varying roundtrip delay, an information feedback based control structure offered the best robust performance characteristics.

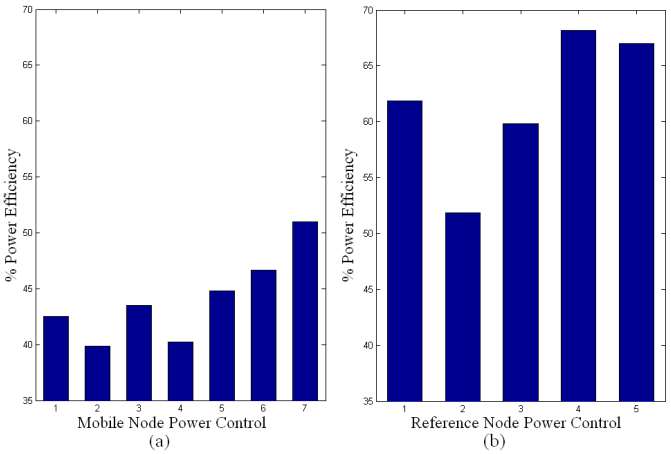

Fig. 9. Power efficiency for each controller configuration where (a) is power efficiency for each of the reference node control configurations and (b) is power efficiency for each of the mobile node power control configurations.

REFERENCES

B. Zurita Ares, C. Fischione, A. Speranzon, and K. H. Johansson. On power control for wireless sensor networks: system model, middleware component and experimental evaluation. *European Control Conference, Kos, Greece*, 2007.

K. Astrom and B. Wittenmark. *Computer Controlled Systems Theory and Design.* Prentice-Hall, Englewood Cliffs, NJ, USA, 3 edition, 1997.

IET Engineering and Technology Magazine. Rescue robots hit comms snag, April 2007.

S. Feldmann, K. Kyamakya, A. Zapater, and Z. Lue. An indoor bluetooth-based positioning system: concept, implementation and experimental evaluation. *ICWN'03, Las Vegas, USA*, June 2003.

F. Gunnarsson and F. Gustafsson. Power control in wireless communications networks - from a control theory perspective. *IFAC World Congress*, 2002.

F. Gunnarsson, F. Gustafsson, and J. Blom. Pole placement design of power control algorithms. *In Proc. IEEE Vehicular Technology Conference, Houston, TX, USA*, May 1999.

A. Salmasi and S. Gilhousen. On the system design aspects of code division multiple access (cdma) applied to digital cellular and personal communications networks. *In Proc. IEEE Vehicular Technology Conference, New York, NY, USA*, May 1991.

IEEE Standard. Wireless lan medium access control (mac) and physical layer (phy) specifications for low-rate wireless personal area networks (lr-wpans). *IEEE Std 802.15.4*, 2006.

K. Yedavalli, B. Krishnamachari, S. Ravula, and B. Srinivasan. Ecolocation: a sequence based technique for rf localization in wireless sensor networks. *Fourth International Symposium on Information Processing in Sensor Networks*, pages 285 – 292, 2005.